GFZ
Helmholtz-Zentrum
POTSDAM

Originally published as:

Sopher, D., Juhlin, C., Huang, F., Ivandic, M., Lueth, S. (2014): Quantitative assessment of seismic source performance: Feasibility of small and affordable seismic sources for long term monitoring at the Ketzin CO2 storage site, Germany. - *Journal of Applied Geophysics*, *107*, p. 171-186.

DOI: http://doi.org/10.1016/j.jappgeo.2014.05.016

Journal of Applied Geophysics 107 (2014) 171–186

Contents lists available at ScienceDirect

Journal of Applied Geophysics

journal homepage: www.elsevier.com/locate/jappgeo

# Quantitative assessment of seismic source performance: Feasibility of small and affordable seismic sources for long term monitoring at the Ketzin $CO_2$ storage site, Germany

Daniel Sopher [a,*], Christopher Juhlin [a,1], Fei Huang [a,2], Monika Ivandic [a,3], Stefan Lueth [b,4]

[a] Uppsala University, Department of Earth Sciences, Villavägen 16, SE-75236 Uppsala, Sweden
[b] Zentrum fuer Geologische Speicherung, Deutsches GeoForschungsZentrum GFZ, Telegrafenberg, 14473 Potsdam, Germany

ARTICLE INFO

*Article history:*
Received 16 December 2013
Accepted 20 May 2014
Available online 29 May 2014

*Keywords:*
Vibsist
Pre-stack analysis
Swept impact (SIST)
Source comparison
Penetration depth
Signal to noise ratio

ABSTRACT

We apply a range of quantitative pre-stack analysis techniques to assess the feasibility of using smaller and cheaper seismic sources, than those currently used at the Ketzin $CO_2$ storage site. Results from two smaller land sources are presented alongside those from a larger, more powerful source, typically utilized for seismic acquisition at the Ketzin. The geological target for the study is the Triassic Stuttgart Formation which contains a saline aquifer currently used for $CO_2$ storage. The reservoir lies at a depth of approximately 630 m, equivalent to a travel time of 500 ms along the study profile. The three sources discussed in the study are the Vibsist 3000, Vibsist 500 (using industrial hydraulic driven concrete breaking hammers) and a drop hammer source.
Data were collected for the comparison using the three sources in 2011, 2012 and 2013 along a 984 m long line with 24 m receiver spacing and 12 m shot spacing. Initially a quantitative analysis is performed of the noise levels between the 3 surveys. The raw shot gathers are then analyzed quantitatively to investigate the relative energy output, signal to noise ratio, penetration depth, repeatability and frequency content for the different sources. The performance of the sources is also assessed based on stacked seismic sections. Based on the results from this study it appears that both of the smaller sources are capable of producing good images of the target reservoir and can both be considered suitable as lower cost, less invasive sources for use at the Ketzin site or other shallow $CO_2$ storage projects. Finally, the results from the various pre-stack analysis techniques are discussed in terms of how representative they are of the final stacked sections.

© 2014 The Authors. Published by Elsevier B.V. This is an open access article under the CC BY-NC-ND license (http://creativecommons.org/licenses/by-nc-nd/3.0/).

## 1. Introduction

Carbon Capture and Storage (CCS) is one of the options available to the global community to reduce $CO_2$ emissions, and hence mitigate climate change in the future. In order to successfully implement CCS it is important to perform an adequate assessment of the suitability of a potential storage reservoir before injection begins. It is also important to monitor the location and size of the injected $CO_2$ plume within the reservoir and detect any potential leakage, during and after injection. These steps, as well as leading to the successful implementation of CCS, are vital in order to meet legislative requirements and build public confidence and acceptance of the technology.

This study was conducted at the Ketzin $CO_2$ storage site located close to the town of Ketzin, west of Berlin, Germany (Fig. 1). The Ketzin $CO_2$ storage site was first established in 2004 (Förster et al., 2006). The injection and observation wells were then drilled in 2007. Injection began at the site in June 2008 and continued until August 2013. During this period 67,271 tons of $CO_2$ were injected into a saline aquifer within the Triassic Stuttgart Formation.

Seismic methods provide one of a range of geophysical methods which can be used to image a $CO_2$ storage reservoir, monitor movement of the injected $CO_2$ within and detect leakage out of it. At the Ketzin site, seismic methods have proven effective at imaging the overall structure and geometry of the reservoir unit (Juhlin et al., 2007). Time lapse surface seismic methods have been applied successfully to monitor and assess the volume of injected $CO_2$ between 2005 and 2009 (22,000 tons of $CO_2$ injected) (Ivanova et al., 2012). Ivandic et al. (2012) used the sparse Star acquisition geometry (Fig. 1) to image the $CO_2$ plume between 2005 and 2011 (45,000 tons $CO_2$ injected). Other examples of the use of seismic methods at Ketzin include work by Zhang et al. (2012) who applied crosshole seismic traveltime and waveform tomography in order to image injected $CO_2$ at Ketzin. Yordkayhun et al. (2009a) used

* Corresponding author. Tel.: +46 18 471 7161; fax: +46 18 501 110.
*E-mail addresses:* daniel.sopher@geo.uu.se (D. Sopher), christopher.juhlin@geo.uu.se (C. Juhlin), fei.huang@geo.uu.se (F. Huang), monika.ivandic@geo.uu.se (M. Ivandic).
[1] Tel.: +46 18 471 2392; fax: +46 18 501 110.
[2] Tel.: +46 18 471 3322; fax: +46 18 501 110.
[3] Tel.: +46 18 4717 157; fax: +46 18 501 110.
[4] Tel.: +49 331 288 1558; fax: +49 331 288 1502.

http://dx.doi.org/10.1016/j.jappgeo.2014.05.016
0926-9851/© 2014 The Authors. Published by Elsevier B.V. This is an open access article under the CC BY-NC-ND license (http://creativecommons.org/licenses/by-nc-nd/3.0/).

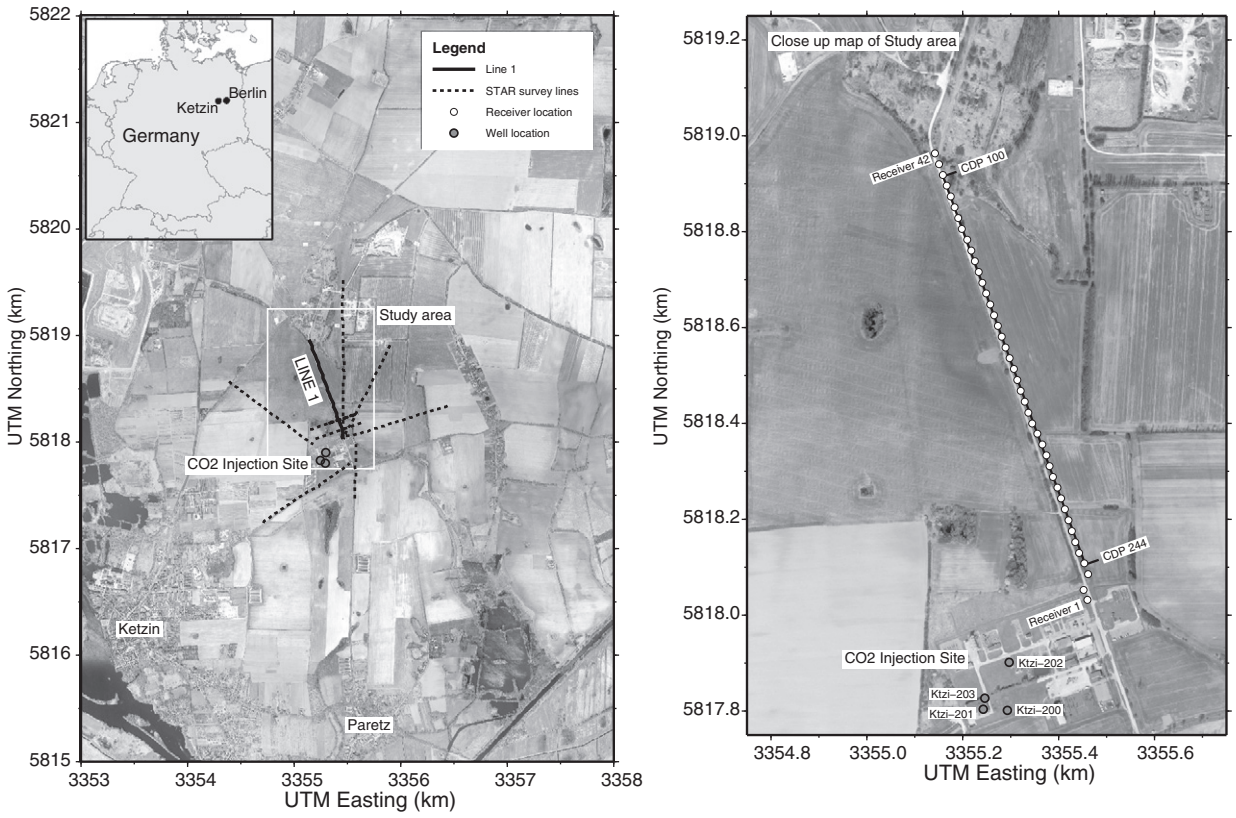


**Fig. 1.** Maps detailing the location of the Ketzin $CO_2$ storage site in Germany, as well as the acquisition geometry for the Ketzin Star survey. A close-up map shows the receiver locations for the study profile as well as the CDP binning line end points. The location of the Ktzi200/2007 well is shown on the close-up map.

3D seismic traveltime tomography to image the shallow subsurface at Ketzin. Zhuo et al. (2012) tested passive seismic interferometry to image the structure at Ketzin. Seismic methods have also been applied successfully to monitor other $CO_2$ storage sites such as Sleipner in the North Sea (Arts et al., 2004) and Weyburn in Canada (White, 2009).

Several different types of seismic sources exist which can provide the input signal for an active seismic survey. The relative performance, advantages and disadvantages of these different sources vary based on the size and mechanism by which they operate. In addition, the chosen target and survey objectives will influence what characteristics are desirable in the source. In general, it is desirable to have a source which can provide a high enough signal strength so that the reflection from the chosen target is higher than the ambient or source generated noise in the seismic record. It is also commonly desirable to have a broad enough bandwidth or frequency content so that the target can be suitably resolved. Choosing an appropriate seismic source is therefore often a crucial decision, which can to a large extent define the overall success of a given seismic survey. The choice of seismic source has a great bearing on the resulting data, affecting amongst other things, the maximum depth which is imaged, signal strength and resolution (Miller et al., 1986). Near surface conditions can also highly affect performance and should be taken into account when choosing a source (Herbst et al., 1998). Practical aspects such as cost, reliability, maneuverability and environmental impact also vary significantly between different seismic sources.

A range of different methods exist to quantitatively assess the performance of a given seismic source. These different methods can be applied to data after stacking, however the main focus of this study is on methods applied to pre-stack data. These methods are intended to provide quantitative measures of a range of factors, such as, signal penetration depth, signal coherency, signal frequency and signal to noise ratio. Note that we use the term penetration depth in this paper in line with previous studies (Barnes, 1994) even though our analysis is performed in the time domain. The depth can be determined from the time domain analysis if the velocity is known. Together, these methods are typically used to provide a quantitative basis for the comparison of different seismic sources, and have been applied in a range of studies (for example Benjumea and Teixidó, 2001; Herbst et al., 1998; Miller et al., 1986). It is also possible to use these methods for real time quality control during seismic data acquisition. This allows variations in the seismic data quality to be monitored due to relative changes in ambient noise, ground conditions or source performance throughout a given survey.

Broadly, seismic sources can be grouped based on the nature of the signal they produce, being either impulsive (e.g. dynamite, weight drop or sledgehammer) or swept (e.g. Vibroseis). Where impulsive sources deliver the source energy in a single pulse, swept sources deliver the energy over many seconds in a controlled manner, which can later be converted to a single wavelet in the data through processing. In this study we discuss data from 3 different land seismic sources. One of the sources (Bobcat with drop hammer) can be considered to be an impulsive source, delivering the signal via a single hammer blow. The other two sources can be considered to be swept sources (Vibsist 3000 and 500), utilizing the Swept Impact Seismic Technique (SIST) (Park et al., 1996). In this method a series of impacts are produced over a period of approximately 20–30 s (termed a Sweep) using a hydraulic hammer. A typical sweep consists of approximately 100–140 hits. During the sweep the time intervals between the hits gradually decrease or increase. During the sweep the time of each hit is recorded via an auxiliary pilot trace. The hit times in the pilot trace are later used to decode the data using the shift and stack process (Park et al., 1996). In this process the entire record is shifted so that the first hit lies at a specified time, for example we consider a time 100 ms from the beginning of the record. A second copy of the same record is then shifted so that the second hit lies at 100 ms, which is then added to the first. This is repeated for

each hit within the sweep. Due to the varying impact interval, the shot is only stacked constructively for a hit at 100 ms.

An accelerated weight drop truck source (impulsive type source) has been used to acquire data for the 3D seismic surveys at Ketzin (Juhlin et al., 2007; Yordkayhun et al., 2009b). This source has performed well, providing a good image of the target reservoir. However, during acquisitions at Ketzin issues have arisen with local landowners concerning tracks left across agricultural land, leading to delays in acquisition and payment of compensation to the landowners. Costs associated with the seismic source also account for approximately 30% of the cost of a typical survey. When considering long term monitoring of CCS projects in general, costs associated with many repeat seismic surveys can be prohibitive. Therefore, the evaluation of cheaper and less invasive sources could be beneficial for long term monitoring at Ketzin as well as other $CO_2$ storage projects.

Here we present a case study of the application of a range of quantitative analysis techniques to data collected using three different seismic sources at the Ketzin $CO_2$ storage site (Fig. 1). The results are used to assess the suitability of the different sources for imaging the $CO_2$ storage reservoir, which lies at a depth of approximately 630 m. Two of these sources, the Vibsist 500 and Bobcat with drop hammer can be considered to be smaller, cheaper and less invasive alternatives to the weight drop truck used for the 3D baseline and monitor surveys at Ketzin. The third source is the Vibsist 3000, a larger more powerful source similar in performance to the accelerated weight drop truck. The data for each source were collected in three separate campaigns between 2011 and 2013. As a result, weather, ground and noise conditions vary between the datasets, as well as certain aspects of the survey design. This makes a true unbiased comparison of the relative performance of the sources impossible. However, after characterizing some of the environmental and logistical differences between the datasets, we discuss indications of the relative performance of the two smaller sources in the results. Finally we consider the results of the various pre-stack analysis techniques alongside the final stacked sections. This allows for a discussion of the relationship between the quantitative pre-stack measurements of the source performance and the final stacked section. In this paper we refer to the drop hammer source as the Bobcat source since a vehicle and drop hammer were rented from this company. However, it is likely that a similar vehicle and drop hammer could have been used from any company providing these services.

## 2. Geological background

The Ketzin site is located on the flank of the Roskow–Ketzin anticline, formed above an Upper Permian Zechstein Salt pillow, which began to flow during the Triassic (Kossow et al., 2000). Intermittent episodes of deformation and uplift due to salt movement occurred throughout the later part of the Triassic, Jurassic and Cretaceous, giving rise to a folded succession of Triassic and Jurassic strata above the anticline (Förster et al., 2006). Cretaceous sediments are absent at the site due to non-deposition or erosion associated with salt related uplift. As a result, Jurassic sediments are overlain unconformably by Oligocene deposits (Förster et al., 2006). Lithologically, the Triassic–Jurassic sequence consists predominantly of sandstones, shales and siltstones.

The reservoir for the storage of $CO_2$ at Ketzin, and hence the target for this investigation, is the Upper Triassic Stuttgart Formation. With an average thickness of 80 m, the fluvial Stuttgart Formation is heterogeneous, containing both high quality sandy channel reservoir facies and poor quality clayey flood plain deposits (Förster et al., 2006). The reservoir lies at a depth of approximately 630 m. Overlying the reservoir formation are the Weser and Arnstadt Formations, consisting of predominantly fine grain marls and mudstones which were deposited in a playa environment (Förster et al., 2006). Within the Weser formation lies an approximately 10–20 m thick anhydrite layer which gives rise to a strong seismic response, termed the K2 reflector (Juhlin et al., 2007).

The Ktzi200/2007 is one of four wells drilled at the $CO_2$ injection site. The Ktzi200/2007 well can be considered representative of the geology along the seismic profile discussed in this study, lying close to the SE end of the profile (Fig. 1). Fig. 2 shows the stratigraphy of the Ktzi200/2007 well alongside the natural gamma, P-wave sonic and density logs (Prevedel et al., 2008). The natural gamma log is shaded by lithology (modified from Ben Norden, pers. comm.). Fig. 2 also displays a zero offset synthetic which was generated using the well logs. To generate the reflectivity series the logs were first median filtered, then blocked at 3 m intervals. A 45 Hz Ricker wavelet was used as this is representative of the frequencies observed in the final stacked sections at the depth of the Stuttgart Formation. A strong seismic response at about 460 ms is generated by the K2 anhydrite layer at about 550 m. Seismic events also correlate well with the Top Sinemurian Formation and Top Exter Formation. The target for this study, the Top Stuttgart Formation, gives rise to a seismic event at approximately 500 ms along the study profile and lies some 42 ms below the strong K2 marker. Fig. 2 also shows subsets of the final stacked sections generated using data acquired with the 3 different seismic sources discussed in this study. The synthetic has not been tied to these seismic sections; instead a bulk shift of 20 ms was applied to the synthetic in order to match the K2 event. Strong events present in the synthetic can be observed on the seismic sections. Note that the location of the seismogram from the real data is about 500 m north of the well location.

## 3. Previous source comparisons

Due to the importance of selecting an appropriate seismic source, there have been many studies into the relative performance of seismic sources for different surface conditions and subsurface targets. Miller et al. (1986, 1992, 1994) summarized a series of source comparisons performed at test sites in New Jersey, California and Texas, respectively. In each of these studies 12 or more shallow seismic sources are compared. Miller et al. (1994) stated that based on these results it is clear that the near surface conditions greatly affect the relative performance of the source and can influence the entire outcome of a comparative study. In dry and hard ground conditions Miller et al. (1994) suggested the use of weight drop sources and in fine-grained, saturated conditions the use of down hole sources, such as buried explosives or guns. Steer et al. (1996) made a comparison of Vibroseis and explosive sources based on deep seismic reflection profiling data acquired along a COCORP profile in the Williston Basin, USA. Juhojuntti and Juhlin (1998) compared the performance of varying sizes of explosive charges in deep reflection data acquired in the Siljan Ring area, Sweden. Herbst et al. (1998) performed a comparison of 14 different seismic sources with a focus on their capability to image shallow Quaternary sediments in northern Germany. In that study, Herbst et al. (1998) highlighted the large differences observed in the signal strength and frequency content as a result of local subsurface conditions and, therefore, stressed the need to consider many shot points when performing a seismic source comparison. Doll et al. (1998) compared the performance of 9 different seismic sources down to a depth of 500 m at a hazardous waste site in Tennessee. Benjumea and Teixidó (2001) performed a quantitative comparison between low-energy explosives and the Seismic Impulse Source System (SISSY) in a glacial application.

A comparison of sources was performed by Yordkayhun et al. (2009b) at the Ketzin $CO_2$ storage site prior to the Ketzin 3D baseline and monitor surveys. In this study the sources were qualitatively and quantitatively compared based on their ability to image the Upper Triassic Stuttgart Formation. In that study, the accelerated weight drop truck, Vibsist and MiniVib sources were compared along two profiles. It was observed that the Vibsist source provided the greatest depth penetration, while the MiniVib provided the least. The MiniVib source was shown to have the highest frequency content within the upper 500 ms. Yordkayhun et al. (2009b) observed that all sources provided a suitable image down to the target reservoir depth (550 ms/630 m).

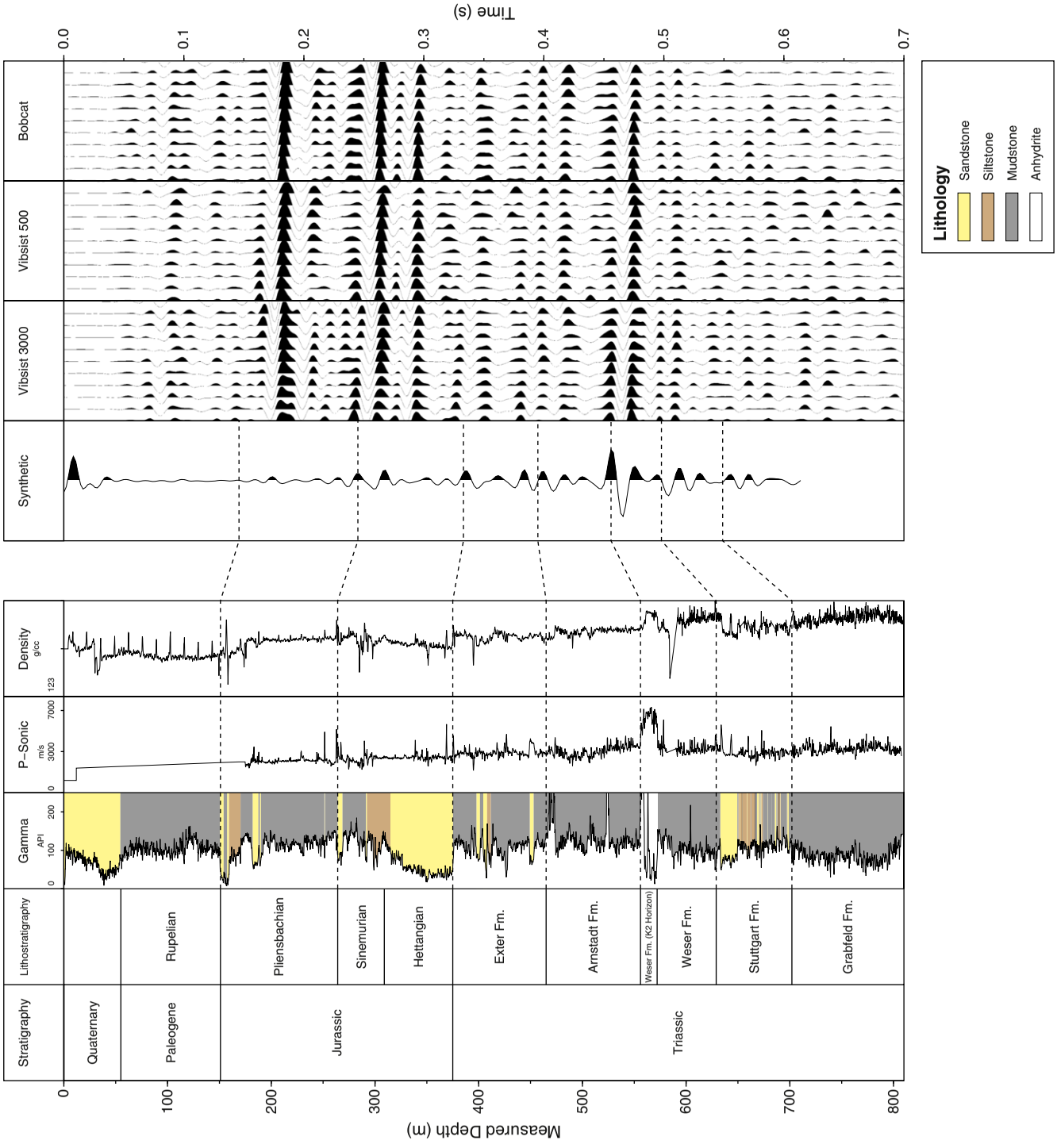
Time (s)
0.0
0.1
0.2
0.3
0.4
0.5
0.6
0.7
Synthetic
Vibsist 3000
Vibsist 500
Bobcat
Lithology
Sandstone
Siltstone
Mudstone
Anhydrite
Density g/cc 1 2 3
P–Sonic m/s 0 3000 7000
Gamma API 0 100 200
Lithostratigraphy
Stratigraphy
Quaternary
Paleogene
Jurassic
Triassic
Rupelian
Pliensbachian
Sinemurian
Hettangian
Exter Fm.
Arnstadt Fm.
Weser Fm. (K2 Horizon)
Weser Fm.
Stuttgart Fm.
Grabfeld Fm.
Measured Depth (m)
0
100
200
300
400
500
600
700
800

**Table 1**
Acquisition parameters for the 3 different surveys.

| Survey | 2011 | 2012 | 2013 |
|---|---|---|---|
| Month | February | November | August |
| Source | Vibsist 3000 | Vibsist 500 | Bobcat drop hammer |
| Impact energy (J/impact) | Up to 3000 | 300–500 | 4882 |
| Impact frequency band (Hz) | 5–250 | 20–1000 | NA |
| Repetition rate (impacts per second) | 1–12 | 3–20 | NA |
| Number of shots (lines 1) | 67 | 71 | 81 |
| Geophones (Hz) | 28 | 28 | 10 |
| Sampling interval (ms) | 1 | 1 | 1 |
| Sweeps | 3 (22 s each) | 3 (22 s each) | 6 hits |
| Receiver spacing (m) | 24 | 24 | 24 |
| Shot spacing (m) | 12 | 12 | 12 |
| Spread length (m) | 984 | 984 | 984 |
| Maximum offset (m) | 916 | 916 | 916 |
| Minimum offset (m) | 5 | 5 | 4 |

### 3.1. Previous data analysis techniques

A range of quantitative methods for comparing the performance of different sources were employed in the studies mentioned in Section 3 which are now discussed. In the studies by Miller et al. (1986, 1992, 1994) the relative total amplitude was calculated by summing the absolute amplitudes along a chosen part of the seismic trace across all traces in a given shot gather, in order to provide a comparison of the energy provided by a source. Herbst et al. (1998) compared the mean square amplitude from a small window within the shot gather where P-wave energy predominates in order to compare the amplitude strength of the generated P-waves. In all of the studies amplitude spectra were used to describe the frequency content of the different sources. Benjumea and Teixidó (2001) and Yordkayhun et al. (2009b) calculated the signal to noise ratio following the method described by Staples et al. (1999). Here the signal to noise ratio was calculated for a given trace by comparing the root mean squared (RMS) amplitude for a window above the first break (noise window) to the RMS amplitude of a window below the first break (signal window). This is described by the equation below:

$$Q_{S/N} = \frac{S_{RMS_{t_0}^{t_0+200\ ms}}}{N_{RMS_{t_0}^{t_0-200\ ms}}} \quad (1)$$

where $Q_{S/N}$ is the signal to noise ratio and $S_{RMS}$ and $N_{RMS}$ describe the RMS amplitude calculated for signal and noise windows, respectively. The first break time is given by $t_0$. In the expression above a 200 ms window for both noise and signal windows is defined.

Quantitative estimates of depth of penetration using seismic reflection data were made by Mayer and Brown (1986), Barnes (1994), Steer et al. (1996), Juhojuntti and Juhlin (1998) and Yordkayhun et al. (2009b). The principle underlying these quantitative methods assumes noise to be constant/stationary and random (Barnes, 1994), leading to a constant background energy in the seismic record. After the activation of the seismic source the energy in the seismic record will first increase and then gradually decrease until a given time when the energy in the trace reaches the background noise level. In this case all energy above the background level is assumed to be due to the source. The point where the energy in the trace reaches the noise level can be considered a measure of the penetration depth of a given source. This is estimated quantitatively by calculating the average absolute amplitude as a function of time from unprocessed shot records (Barnes, 1994; Juhojuntti and Juhlin, 1998; Mayer and Brown, 1986; Steer et al., 1996). Steer et al. (1996), Juhojuntti and Juhlin (1998) and Yordkayhun et al. (2009b) chose to limit the analysis to a given offset range, in order to capture primarily the amplitude of reflected seismic events.

Coherency attributes such as semblance have been discussed in terms of signal and noise energy by Simpson (1967) and Neidell and

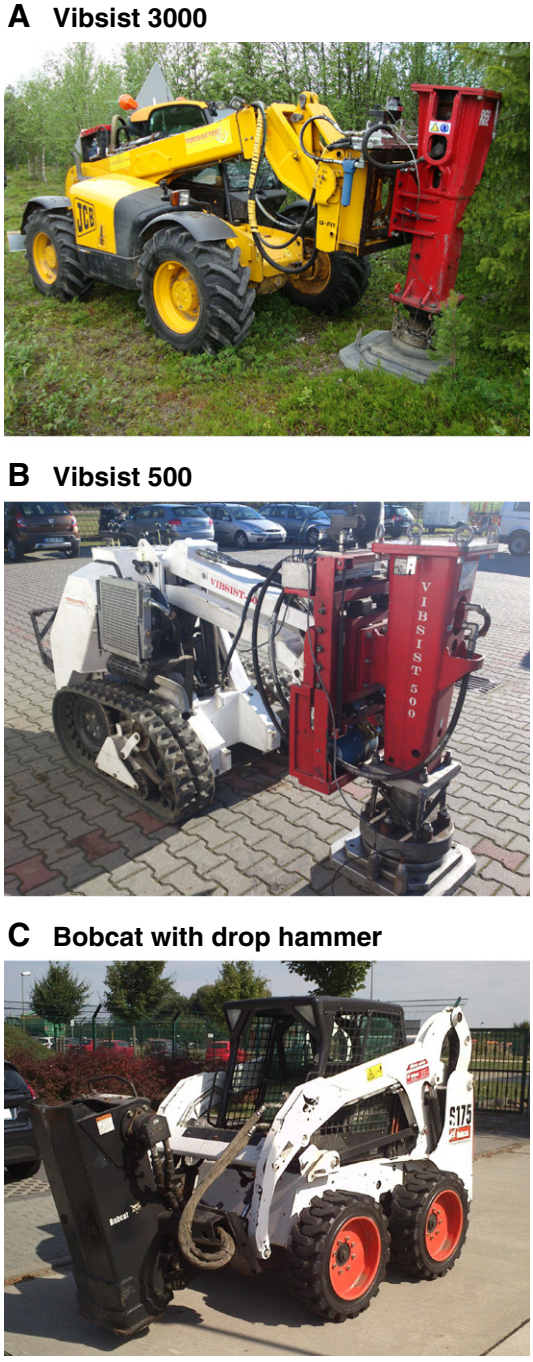


**Fig. 3.** Photos of the three sources used in this study. A). Vibsist 3000 B). Vibsist 500 and C). Bobcat with drop hammer.

**Fig. 2.** Stratigraphy of the Ktzi200/2007 well after Prevedel et al. (2008). P-wave sonic, natural gamma and density logs are also shown. The gamma ray is shaded by lithology based on information provided by Ben Norden (pers. comm). A zero offset synthetic seismogram calculated from the sonic and density logs is shown alongside subsets of the final stacked sections generated using data collected with the 3 different sources. The subsections of stacked data cover the same part of the line for each source, CDP 180 to CDP 190 (approximately 60 m). Dashed lines indicate the position in depth and time of specific well tops. The synthetic has been bulk shifted by 20 ms in order to match the K2 event in the stacked sections.

Taner (1971). The semblance co-efficient ($S_c$) can be calculated as shown below for a given window:

$$S_c = \frac{\sum_{i=1}^{M}\sum_{i'=1}^{M} R_{ii'}(0)}{M\sum_{i=1}^{M} R_{ii}(0)} \quad (2)$$

where $R_{ii'}(0)$ is the zero lag, un-normalized cross correlation between two traces $i$ and $i'$ for the given window of interest. $M$ denotes the number of traces in the multi-trace gather. In typical applications of semblance (i.e. velocity analysis) the window of interest is selected to follow the trajectory of a given reflected event across the gather, calculated for a given zero offset time and stacking velocity. Neidell and Taner (1971) state that if the recorded trace is assumed to be a linear combination of signal and noise and if the noise is random and incoherent, the semblance co-efficient calculated over a given window can be shown to be equal to the ratio of signal energy to total energy. Therefore, if this assumption is valid for the dataset under investigation, the semblance co-efficient can be used as an indicator of the signal strength, relative to the noise.

## 4. Data acquisition

The data for this study were recorded along line 1 of the Star survey (Fig. 1), where data had been collected previously using the Vibsist 3000 in February 2011 (Ivandic et al., 2012). Additional data were collected along line 1 for this study using the Vibsist 500 source in November 2012 and the Bobcat weight drop source in August 2013. The receiver spread for Line 1 of the Star survey is a total of 984 m long, consisting of 42 receivers with 24 m spacing laid out approximately parallel to a road extending north from the $CO_2$ injection site (Fig. 1). Shots were fired with 12 m spacing. Acquisition parameters for the 3 surveys are given in Table 1. Efforts were made to

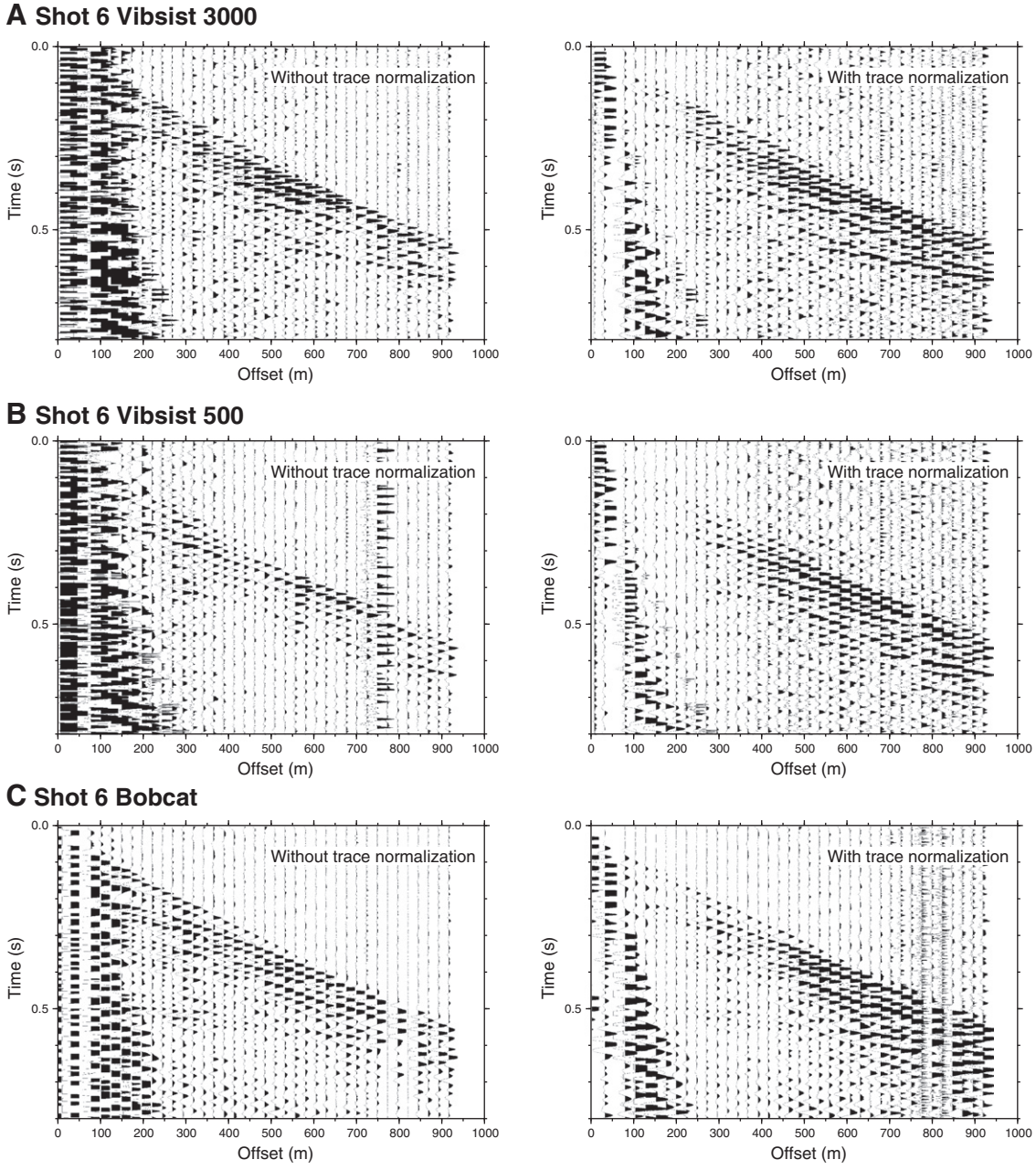


**Fig. 4.** Shot gathers after decoding and stacking of shots for shot point 6. Both normalized and un-normalized gathers are displayed. A). Vibsist 3000 B). Vibsist 500 and C). Bobcat drop hammer. The Bobcat shot gather without trace normalization is scaled differently to the two Vibsist shot gathers.

keep the acquisition parameters and geometries identical between the 3 acquisitions with the exception of the source being used. However, some differences occurred between the different acquisition campaigns and these are described below.

One significant difference is in the shot point locations between the 2013 and the 2011/2012 surveys for the southern end of the line. In the 2011 and 2012 surveys the shot points were located along the receiver line while in 2013 the shot points were located at the side of the road. Therefore, the shot locations for the 2013 survey are offset by approximately 12 m from the shot locations in the 2011 and 2012 surveys at the southern end of the profile. This discrepancy affects approximately 90% of the shots and decreases moving north and disappears at receiver station 35 where the receiver line meets and follows the road (Fig. 1). This means that for the southern part of the line the Vibsist 3000 and Vibsist 500 shots were acquired on plowed agricultural land while the Bobcat shots were acquired on relatively firm grass covered soil beside the concrete road. In 2013, 10 Hz geophones were used as opposed to 28 Hz geophones in 2012 and 2011. This, however, was accounted and corrected for in the subsequent pre-stack analysis and processing. A practical difference between the 3 surveys was that in 2011 and 2012 the data were collected using a wired Sercel seismic acquisition system and in 2013 it was collected using Sercel Unite wireless units. This did not allow for real time quality control of the 2013 data. The near surface conditions varied between the surveys as they were acquired at different times of year. Based on visual assessment, soil moisture levels were highest during the 2011 survey and lowest during the 2013 survey. Kashubin et al. (2011) analyzed differences in the signal to noise ratio and first arrival times between the 2005 baseline and 2009 monitor seismic surveys at Ketzin and concluded that relative changes in precipitation between the two surveys could be linked to relative changes in first arrival time and signal to noise ratio. Based on a visual inspection of the first break pick times between the surveys, the arrival times of the Vibsist 500 and Vibsist 3000 appeared to be comparable while those from the Bobcat appeared to be approximately 6 ms later. An obvious explanation for this would be the difference in shot locations between the Bobcat and Vibsist surveys, however it cannot be ruled out that some component of this is due to differences in the near surface water content between surveys. It is noted in the observer logs that it rained during the acquisition of part of the Vibsist 500 survey; based on the observations by Kashubin et al. (2011) this is likely to have impacted the signal to noise ratio of this survey relative to the other two surveys. Wind conditions were not documented, but are likely to have varied between the three surveys. Therefore, as a result of the varying weather conditions between the acquisitions, the background noise level is likely to vary between surveys.

Images of the 3 sources used in the acquisition are shown in Fig. 3. Three sweeps were stacked per shot point for the 2 Vibsist sources. Each sweep consisted of approximately 100 hits and 140 hits for the Vibsist 3000 and Vibsist 500 respectively. A pilot signal detailing the timing of the individual hits within each sweep was transmitted by radio and recorded in an auxiliary trace for each shot gather. This was later used to decode the data with the shift stack process (Park et al., 1996). Based on the technical specifications, the Vibsist 500 is a smaller, lighter, less powerful and higher frequency source than the Vibsist 3000. The Bobcat drop hammer source consisted of a Bobcat S175 Skid Steer loader with a drop hammer attachment. The drop hammer is a tool for breaking concrete and hence is not specifically designed to perform as a seismic source. A 1 inch thick aluminium plate was used along with the Bobcat drop hammer source for improved coupling. A geophone was attached to the plate, which in turn was connected to a system to record the GPS times of each shot. These GPS times were later used to collect the relevant shot gathers from the wireless units, which were continuously recording in the field. An undesirable feature of the Bobcat source was significant bouncing of the drop hammer after the initial impact on most shots. These bounces, however, did not add constructively when stacking multiple shots and hence are not significant in the final shot gathers. 6 hits were stacked per shot point for the Bobcat drop hammer source. The number of sweeps/hits for each survey was chosen based on acquisition time, so that all shots for the study profile could be acquired in approximately 1 day of shooting. Both the Bobcat drop hammer and Vibsist 500 are smaller and weigh significantly less than the Vibsist 3000.

## 5. Pre-stack comparison

Despite efforts to collect data using exactly the same geometry for all 3 surveys, differences still existed between the shot and receiver points between the three surveys. In addition, some shot points were omitted in some of the surveys. Before proceeding with the study, the shot and receiver locations were compared between all 3 surveys. Receiver and shot locations were only kept if the locations were within 2 m of each other. An exception to this was the large difference in shot locations between 2011/2012 and 2013. In this case shot points were only retained

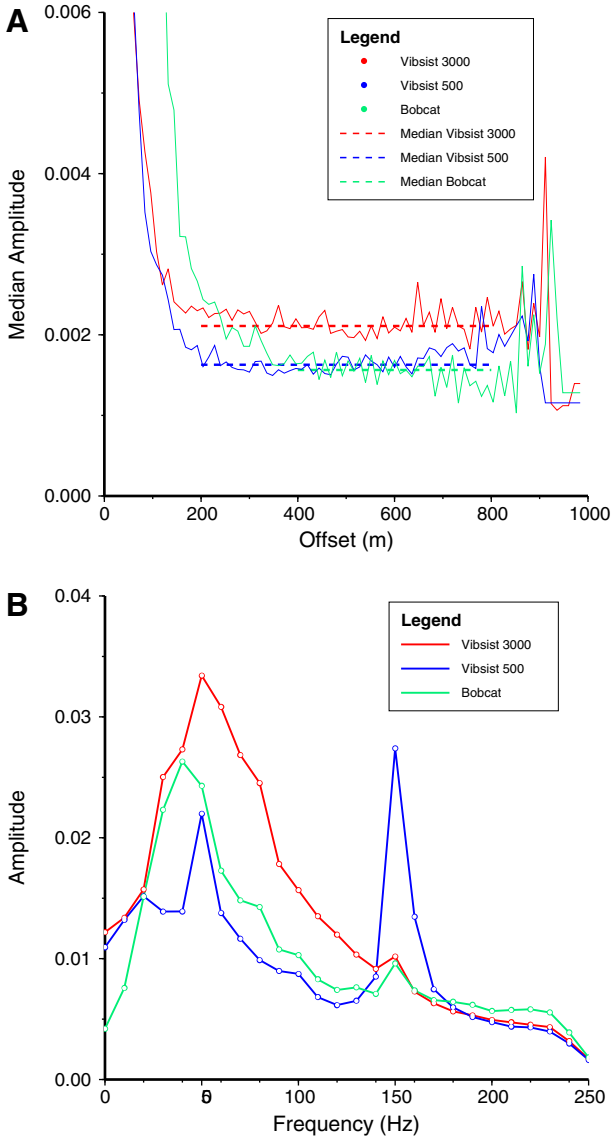


**Fig. 5.** Quantitative noise analysis results performed on raw un-stacked and un-decoded shot gathers. A). Median absolute amplitude in the 100 ms noise window vs. offset. Median average noise amplitude calculated for offsets between 200–800 m and 400–800 m for Vibsist and Bobcat sources, respectively, are shown as dashed lines. B). Amplitude spectra calculated in a 100 ms noise window for the 3 different surveys. Only traces with offsets of 200–800 m and 400–800 m were used to calculate spectra for the Vibsist and Bobcat data, respectively.

if they were located within 12 m of each other. After this process the data from the three different surveys had an equal number of shots, receivers and traces (67 shots, 38 receivers and 2546 traces).

As the 2013 Bobcat drop hammer survey was conducted with 10 Hz geophones a high-pass Butterworth filter and bulk amplitude scaling factor were applied to the data in order to correct the response to be similar to that of a 28 Hz geophone. This correction was applied before any analysis was performed on the gathers.

Observations on shot gathers and the quantitative analysis performed as part of this study show that the shift stack process (Park et al., 1996) significantly alters the noise and signal strength in the data. Despite a significant increase in the signal to noise ratio, both the noise and signal amplitude decreased significantly relative to the original un-decoded data. Therefore, direct comparisons of amplitudes were no longer meaningful between the decoded Vibsist and Bobcat data. In order to compare the Vibsist and Bobcat datasets quantitatively after the decoding process different scaling factors were applied depending on the nature of the comparison, typically the data were scaled relative to the background noise.

Fig. 4 shows images of representative shot gathers from the three different surveys. The shot gather is displayed after decoding (Vibsist data) and stacking of shots; both balanced and unbalanced shots are displayed. Amplitude balancing is performed by equalizing the average amplitude across all traces in the gather. Note that the non-balanced Bobcat shot gather is scaled differently compared to the two non-balanced Vibsist shots. A number of qualitative observations can be made from the raw gathers. Firstly, the ambient noise appears to be lower on the Vibsist 500 data than the Vibsist 3000; similarly the signal strength appears to be lower in the Vibsist 500 data than in the Vibsist 3000 data. The signal to noise ratio appears to be highest for the Bobcat data, where reflections from the K2 horizon at about 500 ms are clearly observable. Conversely the signal to noise ratio appears to be lowest for the Vibsist 500 data. The following sections describe a series of quantitative comparisons which have been made between the different datasets in order to assess the relative performance of the different sources.

### 5.1. Background noise

The qualitative observations of the gathers in Fig. 4 indicate a varying noise level between the different datasets. Therefore, in order to quantitatively compare the three sources it is important to assess the relative background noise levels between the surveys. In order to assess the background noise level, the first 100 ms were analyzed from over 3000 traces from the raw undecoded/unstacked shot gathers. These data were then binned by offset and the median average absolute amplitude was calculated. Fig. 5A shows the median average absolute amplitude vs. offset for the three sources. Mean amplitude and root-mean-square (RMS) amplitude were also calculated, giving trends similar to those observed using the median average. It is important to note, that while it was possible to select a 100 ms window above the first arrivals in the undecoded Vibsist data for all offsets, this was not possible for the Bobcat data, where offset values lower than approximately 150 m are contaminated with signal. The offset noise curves for the Vibsist sources exhibit a noise peak at offsets lower than 200 m, which is interpreted to be source generated noise. As offset increases the effect of this source generated noise diminishes and the curve appears to stabilize at a constant value, which is interpreted to be the background noise level. At offsets beyond approximately 800 m there are relatively few data points, which results in greater variation in the median average. For the Bobcat source, a sharp drop in average amplitude is observed after approximately 150 m, beyond which signal is no longer included in the 100 ms noise window. Between 150 m and 400 m however, there appears to be a gradual decrease in average amplitude which is interpreted to be source generated noise. Beyond approximately 400 m the average noise amplitude for the Bobcat appears to plateau. It appears, therefore, that source generated noise is no longer significant beyond 200 m and 400 m for the Vibsist and Bobcat datasets, respectively. A possible explanation for the apparently more prevalent source generated noise in the Bobcat dataset is the fact that all shots were performed along the road, which could have allowed the source generated noise to propagate along the line more easily.

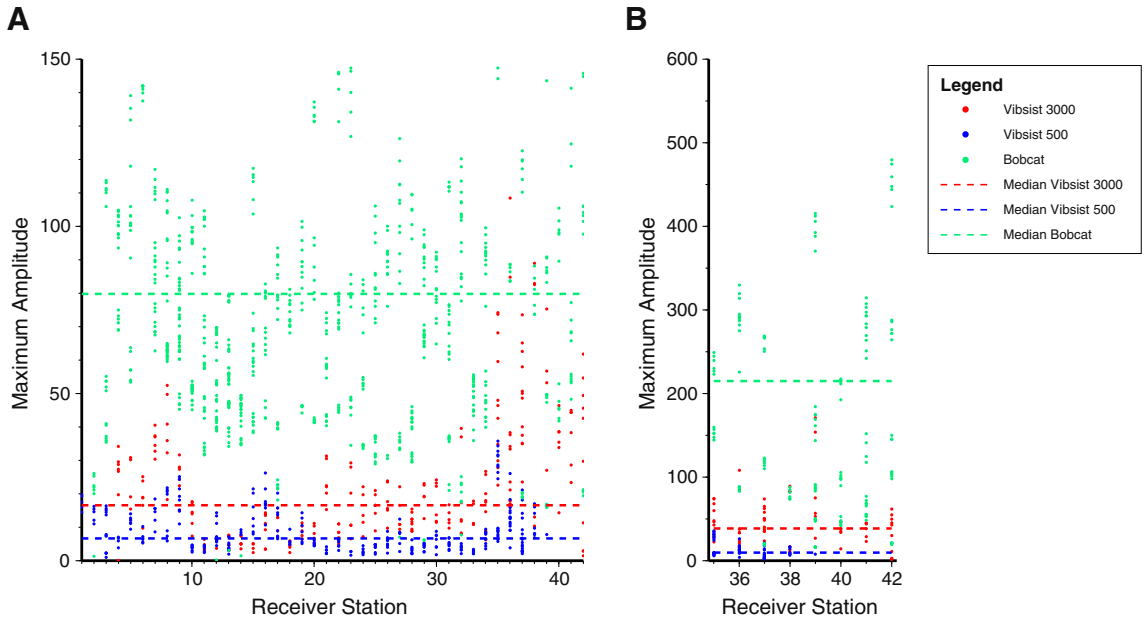


**Fig. 6.** Maximum amplitude from the nearest offset trace for a 400 ms window centered on the first arrival, for each un-stacked/un-decoded shot gather. A). Maximum amplitude for all shots along entire line, for each of the three datasets. Note, vertical scale is such that the highest Bobcat values are omitted. Dashed lines show median average value. B). Maximum amplitude for northern portion of the line, for each of the three datasets. For this portion of the line all three sources had the same shot points located at the side of the road. Dashed lines show median average value.

The median average amplitudes were calculated for the relatively stable portion of each amplitude–offset curve, which were taken to be representative of the background noise level. Based on these results there appears to be different levels of noise for the different surveys. It is clear that the noise is highest in the Vibsist 3000 survey where it is approximately 33% higher than the Vibsist 500 and Bobcat surveys, which appear to have comparable noise levels. If we express the noise levels of the other surveys as a fraction of the noise level in the Vibsist 3000 survey, we can obtain factors of 1, 0.77 and 0.74 which express the relative background noise level for the Vibsist 3000, Vibsist 500 and Bobcat datasets respectively.

Median frequency spectra were also calculated for the 100 ms noise window between offsets of 200–800 m and 400–800 m for the Vibsist and Bobcat datasets, respectively (Fig. 5B). Noise peaks at 50 Hz and 150 Hz are observed in all three datasets, interpreted to be electrical noise. It appears that although the median average noise amplitude for the Bobcat and Vibsist 500 sources is comparable, the typical frequency of the noise in the Bobcat data is far lower than that of the Vibsist 500.

### 5.2. Source energy

As stated in Section 4 we chose the number of sweeps/hits for each shot point based on the practical parameter of acquisition time. However, this choice certainly has implications on the resulting quality of the acquired seismic data. In this section we attempt to quantify the amount of energy each source delivers based on an analysis of the pre-stack data. This allows us to quantify to some degree the effect of our choice of sweep/hit number on the datasets, and to view the results of subsequent data analysis in the context of the relative energy provided by each source. Table 1 details the energy per impact for the three different sources based on information from the equipment providers. Therefore, for a given hit, the Bobcat is expected to provide at least 1.6 times more energy than a hit from the Vibsist 3000 or 10–16 times more energy than a hit from the Vibsist 500. In this study, a given sweep typically contained approximately 100 hits for the Vibsist 3000 and 140 hits for the Vibsist 500. If we therefore consider the energy for a given Vibsist sweep using these values, one would anticipate the total energy to be at least 1 order of magnitude higher than a single hit from the Bobcat. If we consider the qualitative observations of the gathers however this seems counter intuitive.

In order to investigate this further using the seismic data, we first consider that the energy of a wave is proportional to the amplitude of the wave squared, i.e. a 2 fold increase in amplitude is linked to a 4 fold increase in energy. Therefore, the maximum amplitude recorded on the near offset trace, after a given impact, should provide some indication of the relative energy provided by that source. In order to measure this we record the maximum absolute amplitude for the nearest offset trace for a given undecoded/unstacked shot gather, in a 400 ms window centered on the time of an individual source hit. This is then repeated for each shot, for each of the three datasets. The results, sorted by receiver number are shown for both the entire line, and for receivers 35–42 (Fig. 6A and B). As discussed earlier, the shot locations for all three surveys were performed at the same locations along the receiver line, at the side of the road, for receiver stations 35–42. A number of observations can be made from these results. Firstly it is clear that the greatest amplitudes are provided by the Bobcat source, while the lowest are provided by the Vibsist 500 source. If the results for the entire line are considered, it appears that the amplitudes increase for all three sources for receiver stations 35–42. For the Bobcat source this is most likely because the shots were acquired along the road, and as a result

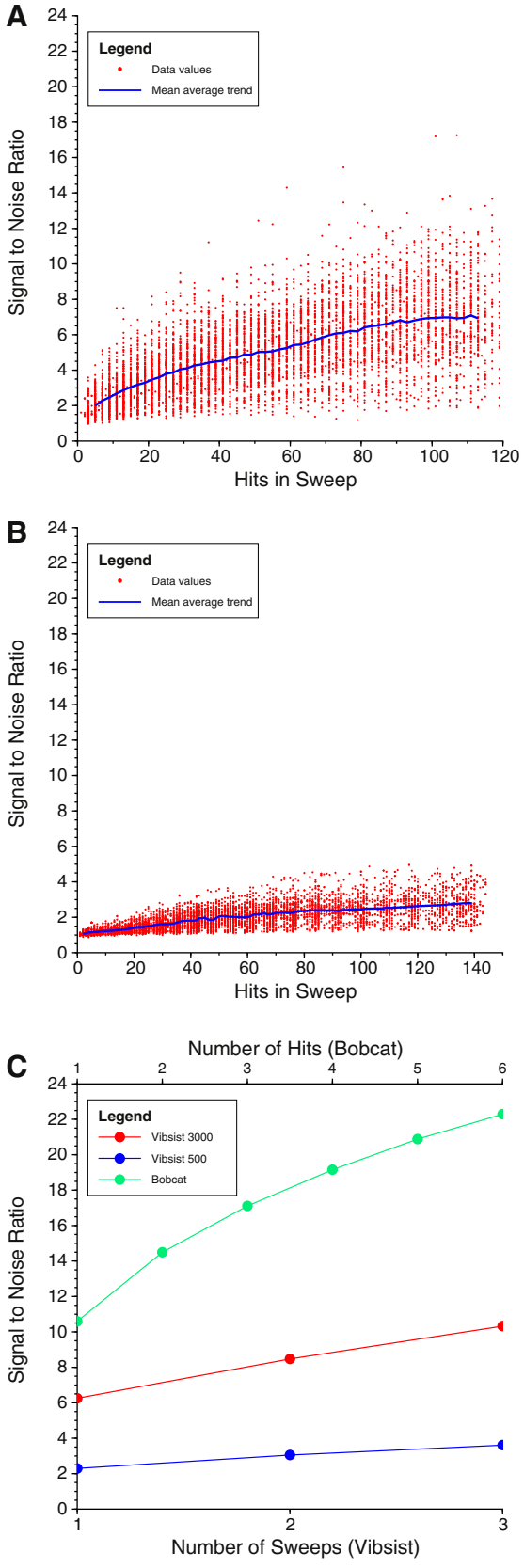


**Fig. 7.** Signal to noise variations during decoding and the shot stacking process. A). Signal to noise vs. number of hits within a sweep calculated for all traces in the dataset for the Vibsist 3000. The blue line indicates the mean average signal to noise ratio vs. number of hits in the sweep. B). Signal to noise vs. number of hits within a sweep calculated for all traces in the dataset for the Vibsist 500. The blue line indicates the mean average signal to noise ratio vs. number of hits in the sweep. C). Signal to noise ratio as a result of stacking multiple shots/sweeps for the Vibsist 500, 3000 and Bobcat drop hammer sources.

the receivers at stations 1–34 were located at a lateral offset of up to 12 m in the adjacent field. For the Vibsist sources, the shots were acquired along the receiver line and therefore were located in the field for receivers 1–34 before joining the road at receiver station 35. This provides a strong indication that the seismic source performance for stations 1–34 for the two Vibsist sources was adversely affected by acquiring the shots in the field as opposed to along the road. The median average maximum amplitudes for receiver numbers 35–42 are: 112, 38 and 8 for the Bobcat, Vibsist 3000 and Vibsist 500 respectively (Fig. 6B). Considering the relationship discussed above, this implies that the energy provided by a single hit from the Bobcat is 8.8 times that of the Vibsist 3000 and 200 times that of the Vibsist 500. These are notably different from the ratios one would achieve from the specifications. If the total energy in the Vibsist sweep is calculated using these data averages, the total energy of 2 Bobcat hits is approximately equivalent to the energy of 3 Sweeps from the Vibsist 500 while one sweep from the Vibsist 3000 is equivalent to six times the amount of energy provided by two bobcat hits. It appears therefore that the relative energy levels stated in the source specifications are not reflected by the maximum amplitudes observed in the recorded seismic data. Factors such as source coupling and near surface conditions could provide potential explanations for this discrepancy.

### 5.3. Signal to noise ratio

The signal to noise ratio was calculated using the same approach as Staples et al. (1999), Benjumea and Teixidó (2001) and Yordkayhun et al. (2009b), where the RMS amplitudes in a window above the first arrivals were compared to those below (Eq. (1)). In order to do this the first breaks were picked manually and 200 ms noise and signal windows were utilized. As mentioned previously, the Vibsist decoding process (shift and stack) gave rise to a significant relative change in the signal and noise amplitudes. In order to gain a better understanding of this process the signal to noise ratio was calculated for the Vibsist 3000 and Vibsist 500 data after stacking successive hits in a given sweep. The signal to noise ratio vs. hits within a sweep for all traces in the Vibsist 3000 and Vibsist 500 datasets are shown in Fig. 7A and B. The signal to noise ratio of the individual Vibsist hits is low, at approximately 2 for the Vibsist 3000 and close to 1 for the Vibsist 500. After stacking approximately 100–140 hits within a sweep this increases to approximately 6.3 and 2.3 for the Vibsist 3000 and Vibsist 500, respectively. Park et al. (1996) considered the noise in a swept impact source record to be a combination of random noise and correlation noise, and stated that only the signal to random noise is reduced by the square root of the number of hits. This is consistent with our observations (Fig. 7A and B), where the signal to noise ratio does not appear to increase as the square root of the number of hits. Fig. 7C shows the signal to noise ratio after stacking successive shots at a given shot point for both the Vibsist and Bobcat sources. The stacking of successive shots leads to an improvement in the signal to noise ratio by a factor close to the square root of the number of hits for the Vibsist 3000 and Bobcat data. The improvement is, however, lower for the Vibsist 500, indicating a greater proportion of coherent noise for this source. The final mean average signal to noise ratios for the 3 datasets using all the raw decoded/stacked shot records are, approximately 22.3, 10.3 and 3.6 for the Bobcat, Vibsist 3000 and Vibsist 500 sources, respectively.

Fig. 8A shows how the calculated median average signal to noise ratio varies as a function of offset for all traces in the 3 datasets. Here the signal to noise ratio is observed to be at a maximum between offsets of 450 and 850 m for the Vibsist 3000 and Bobcat drop hammer sources. Based on these results it appears that the Bobcat drop hammer has the highest signal to noise ratio, while the Vibsist 500 has the lowest signal to noise ratio of the 3 sources.

As mentioned earlier, the shot locations between the Bobcat and Vibsist surveys differed for the southern part of the line. In order to understand the impact of this difference on the signal to noise ratio, the mean average was calculated for shot points 67–74, equivalent to receiver stations 35–42. For these shots the mean average signal to noise ratio for the 3 datasets was approximately 23.4, 9.9 and 2.8 for

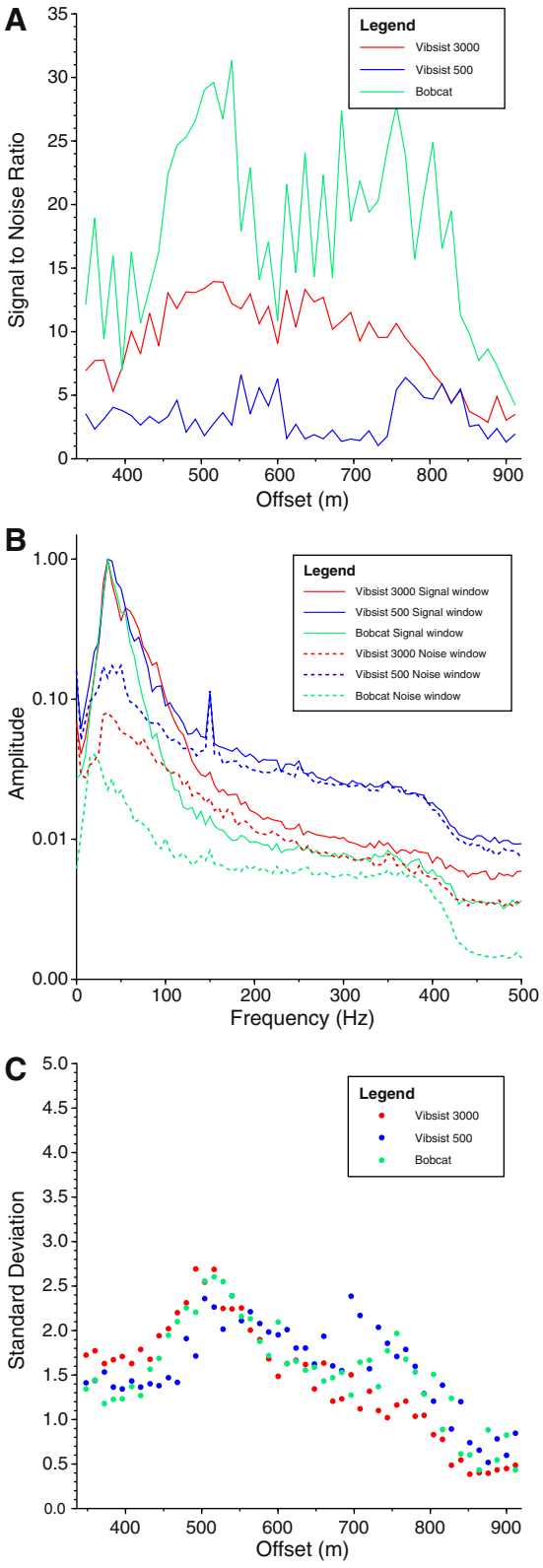


**Fig. 8.** Pre-stack quantitative analysis results. A). Signal to noise vs. offset calculated for all traces on the raw decoded stacked shot gathers. B). Median average amplitude spectra calculated in 200 ms noise and signal windows located above and below the first break time. Solid lines denote the signal spectra, while dashed lines denote the noise spectra. C). Standard deviation vs. offset scaled by the median signal strength for the 3 different sources.

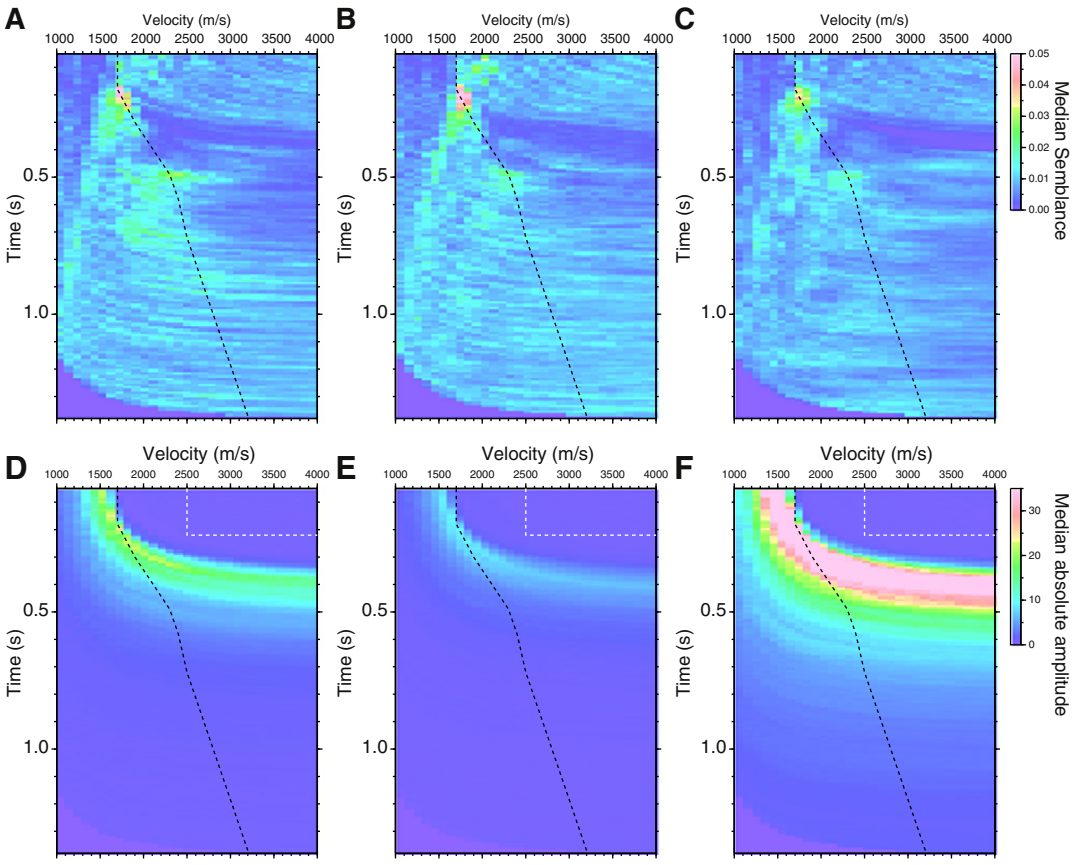


**Fig. 9.** Median average velocity–time–amplitude and median average semblance plots for the 3 datasets. Dashed black line shows the representative velocity trend used to extract the median average curve from the different plots. A), B), and C) show the median average semblance plot for the Vibsist 3000, Vibsist 500 and Bobcat datasets, respectively. D), E), and F) show the median average velocity–time–amplitude plot for the Vibsist 3000, Vibsist 500 and Bobcat datasets, respectively. Area encircled by white dotted line indicates area used to calculate background noise level.

the Bobcat, Vibsist 3000 and Vibsist 500 sources, respectively. These average values are much the same as for the entire line, which indicates that the difference in shot locations did not have a significant effect on the signal to noise ratio.

As discussed in Section 3.1, if certain assumptions about noise and signal in the data are made, the semblance co-efficient can be shown to be equivalent to the signal energy divided by the total energy for a given analysis window (Neidell and Taner, 1971). Semblance coefficients were calculated for all shot gathers using a range of velocities and zero offset times. Only offsets of larger than 500 m were used in order to exclude the high amplitude ground roll and source generated noise. Shot gathers were used in this case, due to the relatively horizontal geology along the study profile. Fig. 9 shows the median average semblance plot for all shots, for each of the three datasets. Fig. 10A shows the median average semblance values extracted along a representative NMO velocity trend. Based on these results it appears that the semblance values for each of the three surveys are very similar. Of the three surveys the Bobcat semblance values are typically slightly lower than the Vibsist values. This could indicate that the signal energy is higher relative to the noise energy for both the Vibsist sources when compared to the Bobcat data. However, it could also indicate that the Vibsist data contain a greater proportion of coherent noise than the Bobcat data.

### 5.4. Frequency content

During the signal to noise analysis the amplitude spectra for the 200 ms noise and signal windows were calculated. These amplitude spectra were averaged across all traces to generate median average noise and signal amplitude spectra for the 3 different sources (Fig. 8B). The spectra were normalized to the peak signal amplitude for each survey and show that the different sources appear to have broadly similar frequency content.

### 5.5. Penetration depth

The penetration depth was calculated for the raw decoded/stacked shot gathers using two different methods. The first method was a modified approach from those adopted by Mayer and Brown (1986), Barnes (1994), Steer et al. (1996), Juhojuntti and Juhlin (1998) and Yordkayhun et al. (2009b). The maximum depth of penetration in these studies was assumed to be the point at which the average amplitude in the traces reaches the background noise level. In order to assess this penetration in the present study all traces in the datasets were grouped by offset. Only offsets greater than 500 m were included as to avoid the influence of surface waves in the analysis. For a given offset group the median absolute amplitude was calculated vs. time. These average amplitude curves were then smoothed using a 31 sample median smoothing filter. These curves were then normalized based on the background noise level of each curve. This was performed by normalizing the average amplitude curves by the average amplitude in the first 200 ms of the curve. The average curves were then normal-moveout (NMO) corrected using a representative velocity function. The final amplitude decay curve was calculated by taking the median average of all the individual amplitude curves, for each offset group. The final amplitude decay curve can be seen in Fig. 10B. The maximum depth of penetration was picked as the point where the average amplitude curve dropped below 110% of the background noise level. This gave a

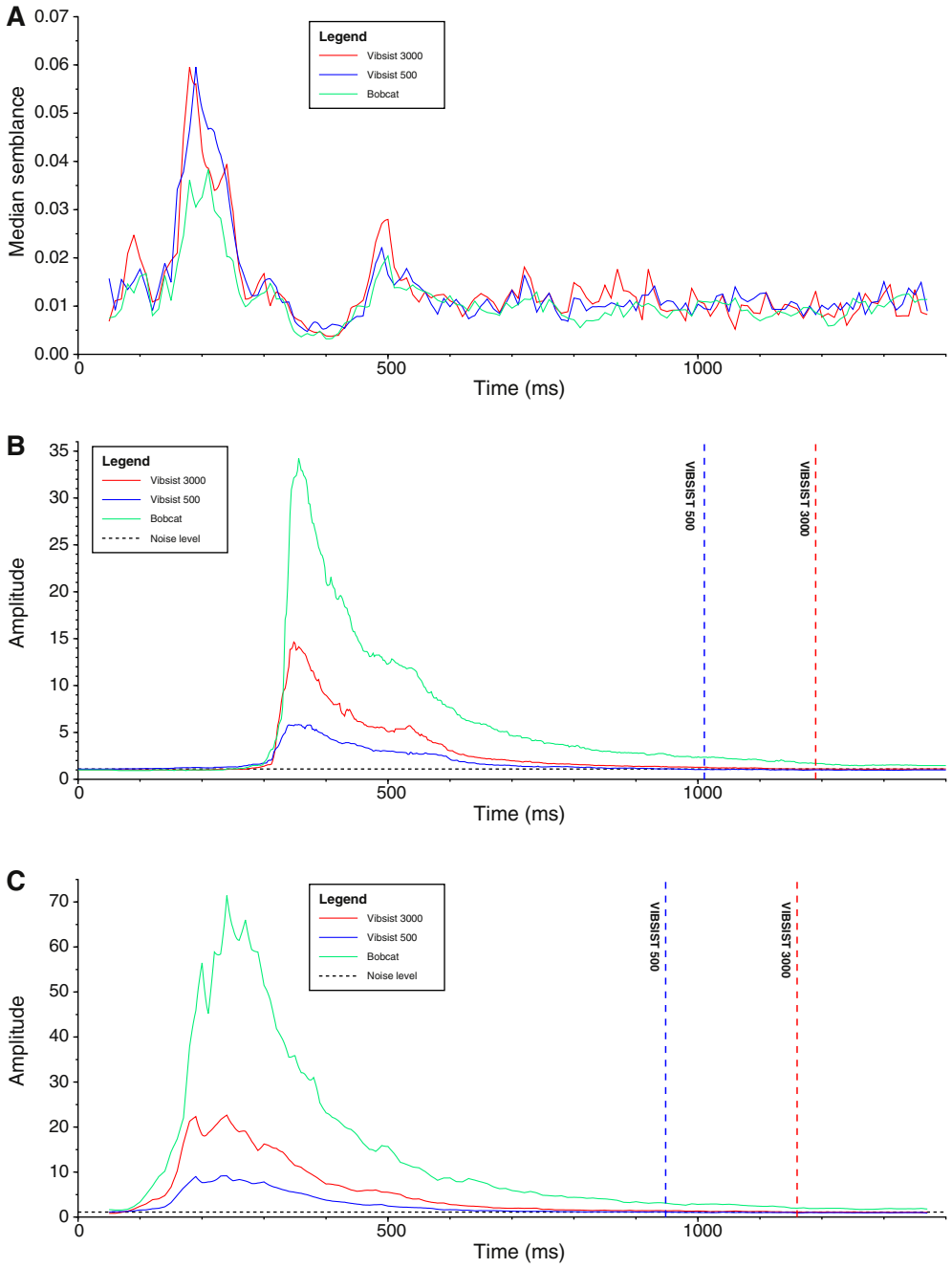


**Fig. 10.** Median average amplitude decay curves and median average semblance curves. A). Median average semblance values extracted along a representative velocity trend for the three datasets. B) and C) show median average amplitude decay curve, calculated using the first and second methods described in Section 5.5, respectively. Dashed lines show the time at which the decay curve drops below 110% of the background noise level.

maximum penetration depth of approximately 1000 ms and 1200 ms for the Vibsist 500 and Vibsist 3000 datasets respectively. The average amplitude depth curve for the Bobcat dataset did not drop below 110% of the noise level for the 1400 ms trace length. Based on these results, the maximum depth of penetration for the Bobcat is therefore inferred to be in excess of 1400 ms.

The second method used to calculate the penetration depth utilizes the same principles as the first, differing only in the way in which the average amplitude decay curves were calculated. In order to calculate the amplitude decay curves the same set of analysis windows defined as part of the semblance analysis were considered (Section 5.3). That is, an analysis window following a trajectory defined by the normal moveout (NMO) across the gather of interest, for a given velocity and zero offset time. However, instead of calculating the semblance coefficient for this window, the absolute amplitude of all samples within the window were summed across all traces in the gather. This was repeated for a range of velocities and zero offset times in order to generate a velocity–time–amplitude plot. This was performed for all shots within the three datasets for offsets greater than 500 m. The median amplitude was then calculated, averaging across all shots in a given dataset. Finally a representative NMO stacking velocity trend was used to extract an amplitude decay curve from the average velocity–time–amplitude plots. These curves were then normalized by the median background amplitude value calculated for a window at the top of the average velocity–time–amplitude plot. Fig. 9 shows the median average velocity–time–amplitude plot for each of the three datasets. The average amplitude decay curve which was extracted for each of the three datasets can be seen in Fig. 10C. In principle, this method should be more

representative of the penetration depth for reflected seismic data, as it is somewhat analogous to stacking the data using a representative NMO velocity function. It is clear however that the results using this method are very similar to those from the first method discussed earlier in this section. If we consider the same threshold criteria to select the maximum penetration depth as above (110% of the background level), we calculate maximum depths of approximately 950 ms and 1150 ms for the Vibsist 500 and Vibsist 3000 sources respectively. In a similar way to the first method, the average amplitude for the Bobcat source does not drop below 110% of the background noise level within the 1400 ms analysis window.

### 5.6. Source repeatability

During the signal to noise analysis, the standard deviation of the RMS amplitude in the 200 ms signal window vs. offset was also calculated for the 3 different surveys. The standard deviation values for each survey were normalized against the median absolute amplitude in the signal window for all traces in that survey. This gives some insight into the relative repeatability of the different sources. The results are shown in Fig. 8C. The analysis shows that relative to the median signal strength, all three sources have a comparable repeatability.

## 6. Post-stack comparison

For post-stack comparison the data were processed using a workflow similar to that used by Juhlin et al. (2007) and Ivandic et al. (2012) (Table 2). All three datasets were processed using the same linear geometry and a 6 m CDP bin size. The initial velocity model for the processing was extracted from the model used by Ivandic et al. (2012) to process the pseudo-3D Star dataset. These velocities were further refined during velocity analysis using constant velocity stacks (CVSs) and gathers (CVGs). The final stacked sections for the 3 different sources are shown in Fig. 11. Subsets of the final stacked sections are also displayed in Fig. 2 where they are compared with the synthetic seismogram. The results show that all sources produce a reasonable and comparable stacked section down to approximately 700 ms, within which the prominent K2 reflection as well as some of the overlying events can be identified and correlated across the section. When considering the portion of the stack from 0 to 700 ms which is dominated by relatively strong and continuous seismic events, these events appear to be most coherent and have the highest amplitudes in the Bobcat data. Within the 0–700 ms interval the events appear to be less coherent and weaker in amplitude with the Vibsist 500 data compared to the other sources. In the deeper part of the stacked section, from 700 to 1400 ms, some weak events can be observed in all stacked sections. These events appear to be most clear on the Vibsist 3000 and Bobcat data. Since the target reservoir lies at a travel time of approximately 500 ms, all sources are capable of imaging the reservoir.

Average amplitude vs. time curves for the stacked sections are also displayed in Fig. 11D. As trace balancing was performed the amplitude decay curves are very similar. However, the amplitudes of the Vibsist 3000 and Bobcat stacks typically appear to be slightly higher than the Vibsist 500 stack. The amplitude spectra for the 3 surveys calculated for the whole stacked section between 400 ms and 700 ms are shown in Fig. 11E. All sources appear to have comparable amplitude spectra in the final stacked sections.

**Table 2**
Workflow used to process seismic data from the 3 different surveys.

| Processing step | |
|---|---|
| 1 | Make geometry: Linear geometry (6 m CDP bins) |
| 2 | Add geometry |
| 3 | Pick first arrivals |
| 4 | Refraction statics |
| 5 | Airwave mute |
| 6 | Butterworth bandpass filter |
| 7 | Spherical divergence |
| 8 | Surface consistent deconvolution — shot domain |
| 9 | Surface consistent deconvolution — receiver domain |
| 10 | Sort to CDP |
| 11 | Apply statics |
| 12 | Calculate and apply residual statics |
| 13 | NMO correction |
| 14 | Trace balance |
| 15 | Stack |
| 16 | FXDECON |

## 7. Discussion

It is clear from the quantitative and qualitative analyses of the pre-stack and stacked data from the test line in this study that the two smaller, more affordable seismic sources are capable of providing a good image of the target $CO_2$ storage reservoir, at the Ketzin site. Results from two different quantitative pre-stack methods utilized in this study indicate that the depth of penetration for both of the smaller sources is approximately 1000 ms or greater. The final stacked sections also show that the target depth of approximately 500 ms is well imaged by both of the smaller seismic sources. The cost difference between the sources cannot explicitly be defined as this is agreed on a contractual basis. However, at the time of these surveys the cost to use two smaller sources was approximately 50%–25% of the cost to use the larger Vibsist 3000 source. Therefore based on these results it seems feasible that small seismic sources such as these could be successfully utilized at the Ketzin site. Therefore, if considering either a single baseline survey, or many surveys as part of a long term monitoring plan, these sources could lead to significant reductions in survey costs. Naturally these small sources would also provide viable options for other shallow investigations, such as other shallow $CO_2$ storage sites, hydrogeological studies and characterization of nuclear fuel storage sites. Small sources such as these could also be used at deeper $CO_2$ storage sites, as a means of detecting and characterizing any leakage of $CO_2$ into shallow aquifers, or the shallow subsurface.

Although an unbiased comparison of the seismic sources is not possible given the differences in the acquisition parameters and ambient conditions, we can make some tentative observations with regard to the relative performance of the two smaller sources. If we consider the results from Section 5.1, the average amplitude of the background noise appears to be comparable for the Bobcat and Vibsist 500 sources, therefore direct comparison of results which have been normalized by the background noise is to some extent reasonable. Based on the results from this study it would appear that the depth of penetration and signal to noise ratio are significantly higher for the Bobcat source. It can also be observed from the stacked sections that the Bobcat data appear to be higher in amplitude and exhibit more continuous seismic events than the Vibsist 500. The semblance results, however, indicate a far smaller difference between the two smaller sources in terms of the signal energy relative to the noise energy. If we consider the relative energy output of the two smaller sources, the 6 hits used in this study for the Bobcat provide approximately triple the energy of the 3 sweeps from the Vibsist 500. It can also be observed from the stacked sections and various pre-stack analysis results that the Vibsist 500 and Bobcat performed well when compared to significantly larger and more powerful Vibsist 3000 source. However, it should be noted that the background noise at the time of the Vibsist 3000 survey was some 33% higher than that of the Bobcat and Vibsist 500 surveys.

When considering the relative performance of the sources it is important to note the variation in ground conditions due to the different seasons in which the datasets were collected. It has been observed that weight drop or hammer type sources appear to perform better when soil conditions are drier (Miller et al., 1994). Therefore the Bobcat survey was acquired with the most favorable surface conditions, on firm grass covered soil, at the end of a dry summer. Muddy and wet

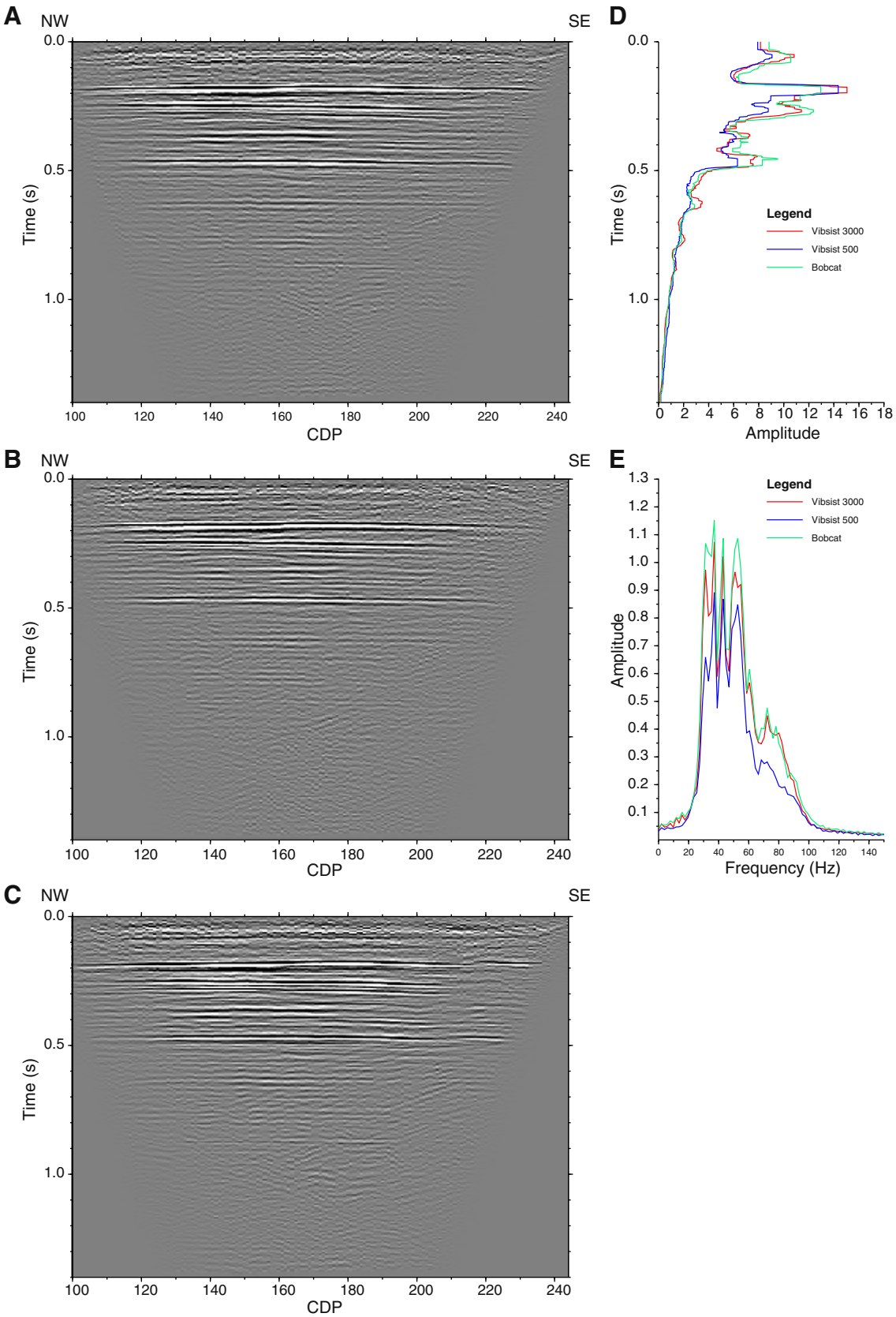


**Fig. 11.** Stacked sections and associated analysis results for the 3 different sources. A). Stacked section for Vibsist 3000 source. B). Stacked section for Vibsist 500 source. C). Stacked section for Bobcat drop hammer source. D). Average absolute amplitude with depth curves for the stacked data. E). Amplitude spectra for the whole stacked section taken between 400 ms and 700 ms.

conditions during the acquisition of the Vibsist 500 survey may have negatively impacted the performance of the source. Rain during acquisition may have acted to further reduce the signal to noise ratio for the Vibsist 500 survey. The difference in shot point locations for the Bobcat source should also be considered. Based on the results of this study, the transition of shot points from the field to the roadside appears to have affected the maximum recorded amplitude in the data for the Vibsist sources. However, this transition appears to have no significant effect on the calculated signal to noise ratios.

In terms of the level of invasiveness of the 3 sources, the Vibsist 500 and Bobcat drop hammer sources are both significantly smaller and lighter than the Vibsist 3000. Based on visual inspection, the size and depth of the tracks left by the smaller sources were reduced compared to the Vibsist 3000. Therefore, it is reasonable to conclude that the smaller sources are less invasive and in the case of Ketzin, would be less disruptive to farming activities in the area. In terms of the maneuverability of the three sources the larger Vibsist 3000 is the most capable of negotiating the muddy field conditions present in the farming areas surrounding the injection site. The Vibsist 500 which uses caterpillar tracks was also able to maneuver through the field to acquire shots along the receiver line. The Bobcat however was not tested in the field due to concerns that it would get stuck if muddy conditions were to arise, as a result shots were only acquired along the road side.

One significant advantage of the various pre-stack analysis methods we have applied is that they can be applied rapidly and with relatively small amounts of data. Making them easy to utilize for real time data quality control or in source comparison studies where there is insufficient data to generate a reasonable stacked section. In the majority of applications the stacked seismic data is the desired product from a given seismic survey. It is therefore interesting to understand the link between the results from these various pre-stack analysis techniques and the quality of the final stacked section. In this study, as both are available, it is possible for us to make a comparison between the pre-stack analysis results and the final stacked sections. If we consider the signal to noise ratios discussed in this study, we observe a very large difference in the calculated values for the three different sources used. Based on the pre-stack analysis the signal to noise ratio of the Bobcat source is typically double that of the Vibsist 3000 and 8 times higher than the Vibsist 500. From these results one would anticipate a marked difference in the stacked sections. However, although the stacked results vary in quality to some extent, they do not vary to this degree. If one considers the method of Staples et al. (1999), it is clear that not all seismic events within the 200 ms signal window are coherent reflected events. For example, refracted seismic events are clearly present within this window in the data for this study, which can be considered to be noise when generating the final stacked section. The signal to noise ratio results generated by this method therefore provide some guide as to the relative signal strength, but should not be considered fully representative of the true ratio of reflected seismic signal to noise in the dataset. The use of semblance as an indicator of the ratio of the signal energy to the total energy does not appear to give results which correspond well to the final stacked results. Here the Vibsist 500 dataset has a higher average semblance value than the Bobcat dataset, but the latter appears to have a better image in the stacked section. This is most likely due to the assumption that noise and signal are independent and that the noise is incoherent in semblance calculation (Neidell and Taner, 1971). It is therefore likely that coherent noise introduced as part of the shift and stack process for the Vibsist 500 dataset, for example, increases the semblance value without leading to an improved stacked image. In this study there is good agreement between two different pre-stack methods for calculating the maximum penetration depth in the seismic data, where the Vibsist 500 and Vibsist 3000 datasets are assigned maximum depth penetrations of approximately 975 ms and 1175 ms respectively. Assignment of a maximum depth of penetration from the stacked section is somewhat subjective, however, the maximum penetration depths from the pre-stack analysis seem reasonable on inspection of the stacked section. The Bobcat results, however, cannot be assessed, as the maximum penetration depth is calculated to be below the maximum time of the stacked section.

## 8. Conclusions

A range of different pre-stack analysis techniques are utilized in order to quantitatively compare the data from the three different surveys. It is clear when considering the final stacked section that some of the pre-stack analysis results can be more closely related to the final stacked section than others. While estimates of the maximum depth of penetration from the pre-stack data used in this study appear to show good correspondence to the final stacked section, estimates of the signal to noise ratio bear a somewhat weaker correlation. Despite these limitations however, in the absence of stacked seismic data, it appears that these pre-stack data analysis methods can provide useful indications about the relative quality of a given seismic dataset.

Two smaller, more affordable seismic sources have been tested at the Ketzin $CO_2$ storage site. The results have been compared quantitatively and qualitatively to a larger seismic source of a similar size and cost to those currently used for seismic surveys at the Ketzin site. Based on the pre-stack data analysis and stacked sections, it is clear that a good image of the target $CO_2$ storage reservoir can be achieved using either of the two smaller sources. It therefore appears feasible that small sources such as these could be used to monitor the reservoir at the Ketzin site, or other shallow $CO_2$ storage sites, leading to significant survey cost reductions. These sources could also be used for a range of other investigations focusing on depths down to approximately 800 m, for example, detection of CO2 leakage at deeper storage sites, hydrogeological studies and characterization of spent nuclear fuel storage sites.

## Acknowledgments

The Swedish Research Council (VR) partly funded Daniel Sopher during this research (project number 2010-3657) and is gratefully acknowledged. The Swedish Energy Authority partly funded the data acquisition (Project No. 35406-1). GLOBE ClaritasTM under license from the Institute of Geological and Nuclear Sciences Limited, Lower Hutt, New Zealand was used to process the seismic data. The European Commission is gratefully acknowledged for their funding of the '$CO_2$CARE — $CO_2$ Site Closure Research, Project No. 256625'. Part of this work has been funded by the European Commission and a consortium of industrial partners consisting of RWE, Shell, Statoil, TOTAL, Vattenfall and Veolia (Project $CO_2$CARE, No. 256625). We would like to thank M. S. Craig and another anonymous reviewer for their valuable input which helped to improve the quality of the manuscript.

## References

Arts, R., Eiken, O., Chadwick, A., Zwegel, P., van derMeer, B., Zinszner, B., 2004. Monitoring of $CO_2$ injection at Sleipner using time-lapse seismic data. Energy 29, 1383–1392.
Barnes, A.E., 1994. Moho reflectivity and seismic signal penetration. Tectonophysics 232, 299–307.
Benjumea, B., Teixido, T., 2001. Seismic reflection constraints on the glacial dynamics of Johnsons Glacier, Antarctica. J. Appl. Geophys. 46, 31–44.
Doll, W.E., Miller, R.D., Jianghai, X., 1998. A noninvasive shallow seismic source comparison on the Oak Ridge Reservation, Tennessee. Geophysics 63, 1318–1331.
Förster, A., Norden, B., Zinck-Jørgensen, K., Frykman, P., Kulenkampff, J., Spangenberg, E., Erzinger, J., Zimmer, M., Kopp, J., Borm, G., Juhlin, C., Cosma, C., Hurter, S., 2006. Baseline characterization of the $CO_2$SINK geological storage site at Ketzin, Germany. Environ. Geosci. 13, 145–161.
Herbst, R., Kapp, I., Krummel, H., Lück, E., 1998. Seismic sources for shallow investigations: a field comparison from Northern Germany. J. Appl. Geophys. 38, 301–317.
Ivandic, M., Yang, C., Lüth, S., Cosma, C., Juhlin, C., 2012. Time-lapse analysis of sparse 3D seismic data from the $CO_2$ storage pilot site at Ketzin, Germany. J. Appl. Geophys. 84, 14–28.
Ivanova, A., Kashubin, A., Juhojuntti, N., Kummerow, J., Henninges, J., Juhlin, C., Lüth, S., Ivandic, M., 2012. Monitoring and volumetric estimation of injected $CO_2$ using 4D

seismic, petrophysical data, core measurements and well logging: a case study at Ketzin, Germany. Geophys. Prospect. 60, 957–973.
Juhlin, C., Giese, R., Zinck-Jrgensen, K., Cosma, C., Kazemeini, H., Juhojuntti, N., 2007. 3D baseline seismics at Ketzin, Germany: the $CO_2$SINK project. Geophysics 72, B121–B132.
Juhojuntti, N., Juhlin, C., 1998. Seismic lower crustal reflectivity and signal penetration in the Siljan Ring area, Central Sweden. Tectonophysics 288, 17–30.
Kashubin, A., Juhlin, C., Malehmir, A., Lüth, S., Ivanova, A., Juhojuntti, N., 2011. A footprint of rainfall on land seismic data repeatability at the $CO_2$ storage pilot site, Ketzin, Germany. 81st Annual International Meeting, SEG, Expanded Abstracts.
Kossow, D., Krawczyk, C., McCann, T., Strecker, M., Negendank, J.F.W., 2000. Style and evolution of salt pillows and related structures in the northern part of the Northeast German Basin. Int. J. Earth Sci. 89, 652–664.
Mayer, J.R., Brown, L.D., 1986. Signal penetration in the COCORP Basin and Range-Colorado plateau survey. Geophysics 51, 1050–1055.
Miller, R.D., Pullan, S.E., Waldner, J.S., Haeni, F.P., 1986. Field comparison of shallow seismic sources. Geophysics 51, 2067–2092.
Miller, R.D., Pullan, S.E., Steeples, D.W., Hunter, J.A., 1992. Field comparison of shallow seismic sources near Chino, California. Geophysics 57, 693–709.
Miller, R.D., Pullan, S.E., Steeples, D.W., Hunter, J.A., 1994. Field comparison of shallow P-wave seismic sources near Houston, Texas. Geophysics 59, 1713–1728.
Neidell, N.S., Taner, M.T., 1971. Semblance and other coherency measures for multichannel data. Geophysics 36 (3), 482–497.
Park, C.B., Miller, R.D., Steeples, D.W., Black, R.A., 1996. Swept impact seismic technique (SIST). Geophysics 61, 1789–1803.
Prevedel, B., Wohlgemuth, L., Henninges, Krüger, K., Norden, B., Förster, A., 2008. The $CO_2$SINK boreholes for geological storage testing. Sci. Drill. 6, 32–37.
Simpson, S.M., 1967. Traveling signal-to-noise ratio and signal power estimates. Geophysics 32 (3), 185–493.
Staples, R.K., Hobbs, R.W., White, R.S., 1999. A comparison between airguns and explosives as wide-angle seismic sources. Geophys. Prospect. 47, 313–339.
Steer, D.N., Brown, L.D., Knapp, J.H., Baird, D.J., 1996. Comparison of explosive and vibroseis source energy penetration during COCORP deep seismic reflection profiling in the Williston Basin. Geophysics 61, 211–221.
White, D., 2009. Monitoring $CO_2$ storage during EOR at the Weyburn-Midale Field. Lead. Edge 28, 838–842.
Yordkayhun, S., Tryggvason, A., Norden, B., Juhlin, C., Bergman, B., 2009a. 3D seismic traveltime tomography imaging of the shallow subsurface at the $CO_2$SINK project site, Ketzin, Germany. Geophysics 74, G1–G15.
Yordkayhun, S., Ivanova, A., Giese, R., Juhlin, C., Cosma, C., 2009b. Comparison of surface seismic sources at the $CO_2$SINK site, Ketzin, Germany. Geophys. Prospect. 57, 125–139.
Zhang, F., Juhlin, C., Cosma, C., Tryggvason, A., Pratt, G., 2012. Cross-well seismic waveform tomography for monitoring $CO_2$ injection: a case study from the Ketzin Site, Germany. Geophys. J. Int. 189, 629–646.
Zhuo, X., Juhlin, C., Gudmundsson, O., Zhang, F., Yang, C., Kashubin, A., Lüth, S., 2012. Reconstruction of subsurface structure from ambient seismic noise: an example from Ketzin, Germany. Geophys. J. Int. 189, 1085–1102.